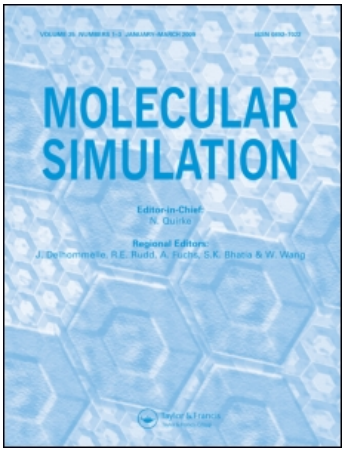

Molecular Simulation
Publication details, including instructions for authors and subscription information:
http://www.informaworld.com/smpp/title~content=t713644482

Host-Dopant Interactions in Ion-Doped Polymers

J. Corish[a]; V. C. A. Hanratty[ab]; D. A. Morton-blake[a]; F. Bénière[c]
[a] Department of Chemistry, Trinity College, Dublin, Ireland [b] Department of Chemistry, Dublin City University, Dublin, Ireland [c] Laboratoire de 'Sciences des Matériaux', Université de Rennes, Rennes, France

To cite this Article Corish, J. , Hanratty, V. C. A. , Morton-blake, D. A. and Bénière, F.(1992) 'Host-Dopant Interactions in Ion-Doped Polymers', Molecular Simulation, 9: 1, 65 — 79
To link to this Article: DOI: 10.1080/08927029208048262
URL: http://dx.doi.org/10.1080/08927029208048262

Molecular Simulation, 1992, Vol. 9, pp. 65–79
Reprints available directly from the publisher
Photocopying permitted by license only

HOST-DOPANT INTERACTIONS IN ION-DOPED POLYMERS

J. CORISH, V.C.A. HANRATTY[1] AND D.A. MORTON-BLAKE†

Department of Chemistry, Trinity College, Dublin 2, Ireland

and

F. BÉNIÈRE

Laboratoire de 'Sciences des Matériaux', Université de Rennes, F-35042 Rennes, France

(*Received September 1991, accepted November 1991*)

Lattices of potassium-doped polyacetylene (PA) and lithium-doped polyparaphenylene (PPP) are simulated employing full lattice relaxation. The polymer chains lose their planar conformations if the symmetry of the unit cell is lowered from that corresponding to the formal analytical compositions e.g., $[CHK_{0.25}]$, $[CHK_{0.125}]$ and $[C_6H_4Li_{0.5}]$. In the K-doped PA lattices the K^+ ions are sufficiently mobile to render a vacancy in their ranks unstable. Results of the defect calculations in K-doped PA suggest that the host and dopant sublattices are incommensurate but that more than one dopant spacing could co-exist in the lattice. In Li-doped PPP, however, the Li^+ ions are more strongly attached to their sites, so that when displaced off their sites the ions generate a degree of local disruption of both sublattices.

KEY WORDS: Conductive polymers, atomistic lattice simulation, ion-doped polyacetylene, ion-doped polyparaphenylene, ionic migration

1 INTRODUCTION

The near-metallic conductivities of ion-doped conjugated polymers and the reversibility of the doping/undoping processes confer interesting properties on these systems which make them candidates for application in electronic devices such as 'plastic batteries' [1–4].

The unavailability of single crystals of the conductive polymers or of their ion-doped products precludes the determination of their complete crystal structures using diffraction methods. Those structures which have been proposed hitherto are limited to polyacetylene (PA) and polyparaphenylene (PPP) and are the results of the interpretations of diffractograms of films and powders [5–10]. While these have furnished lattice vectors and some repeat distances, the atomic positions have been inferred only by performing crystal-packing calculations for which assumptions are made about the geometry of the host polymer sublattices.

Atomistic simulation calculations show that even in the pristine lattices there is a coupling between the distortions of the polymer chains from their isolated-chain geometries and their relative orientations in the unit cell [11]. Doped polymers show

[1]Present address: Department of Chemistry, Dublin City University, Dublin 9, Ireland.
†Author for correspondence.

additional distortions arising from interactions between host and dopant sublattices [12]. In a recent preliminary report [13] we described static lattice simulation calculations using the defective-lattice simulation program CASCADE [14]. These showed that the chain geometry responded to various defects in the K^+ dopant channel by adopting a corrugation of the polymer planes. The present work considers how the motion of the ions in the dopant sublattice of PA and PPP modifies the geometries of the host polymers.

2 POTASSIUM-DOPED POLYACETYLENE

2.1 *Perfect Lattice Calculations*

Although PA can be doped by all alkali metals we have selected potassium as dopant for this investigation, in order to gain from the rather greater amount of experimental data that is available for this doped lattice [5–8]. While lithium might be a good choice for comparison with doped polyparaphenylene in Section 3, the structural parameters for the PALi have not been determined, and there is reason to believe that the system is amorphous [5].

The channel lattice of K-doped PA were simulated using the potential functions reported previously [11, 12] to describe the bonded C–C and C–H stretching interactions, the CCC and CCH bond angle deformations and the non-bonded interactions involving C, H and K atoms. Having shown that in the electrostatic limit the K^+ sites are rather insensitive to a number of proposed electron distributions [12], the simplest distribution – that which would be obtained if the valence electron from each dopant atom were completely transferred to the PA sublattice and distributed evenly among all the carbon atoms – was chosen for the calculations.

Although the diffraction investigations conclude that the dopant ions form linear arrays along the channel axis [5, 7], neither the location of K^+ sites nor their separations have been determined unambiguously. The maximum measured doping level [15] corresponds to the chemical composition $[CHK_{0.18}]_x$. This composition suggests that all the dopant channels are occupied by K^+ ions; however the lack of homogeneity cautions against assigning a K^+ ion to approximately every third C–C link along the polymer chain as would be implied by the composition if the doping were uniform. Since at least some degree of bond alternation is now believed to remain in the PA carbon backbone after doping [16] these calculations consider the two simplest models in which all dopant sites are equivalent. These structures, shown in Figure 1, are (i) that in which a dopant ion is associated with every (formal) ethylenic link, which we term "fully doped PA" or PAK1, and (ii) one in which the K^+ ions are at alternate C=C segments, which structure we shall refer to as "semi-doped PA" or PAK2. Although the chemical analysis of potassium-doped PA has not hitherto found a composition corresponding to the more highly doped of these structures PAK1, nevertheless such a doping level has been found in the sodium doped system whose analysis yielded the "ideal" composition $[CHNa_{0.25}]_x$.

In our earlier simulations of the PAK1 and PAK2 lattices [12] we adopted unit cells (Figure 1) which respectively contained 2 and 4 CH units per chain. A total relaxation of both lattices (including both bonded and non-bonded interactions) resulted in stable structures in which each K^+ ion was equidistant from two carbon atoms in each of the four polymer chains surrounding the channel. These atoms thus formed a serrated ring of 8 carbons surrounding the dopant ion. Any relative displacement of

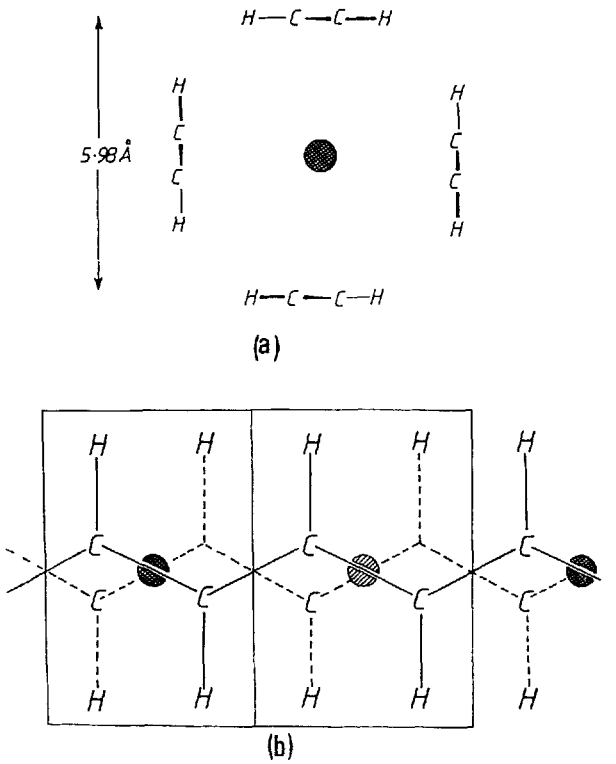

Figure 1 The dopant channel in potassium-doped polyacetylene (PA). (b) The unit cells of fully-doped polyacetylene PAK1 (left hand rectangle only) and of semi-doped polyacetylene PAK2 (large rectangle). In PAK2 the shaded K^+ ion in the right hand rectangle is absent.

host and dopant sublattices followed by lattice relaxation resulted in restoration of the original structure in which the K^+ ions were positioned over the centres of the C–C bonds. Both structures thus appeared to be stable, and the lattice relaxed to polymer conformations which were close to planar.

2.2 *Defect Lattice Calculations: K^+ Vacancy*

The relaxations of PAK1 and PAK2 as the lattices responded to a defect were calculated by the Mott-Littleton 2-region strategy [17] in which Region I in each case contained a total of ~ 150 atoms.

The case in which the defect consisted of a single K^+ vacancy was considered first. The results of the calculation showed that although the bond lengths and bond angles in the host polymer are retained to within 2% of their values in the perfect lattices, both structures exhibit conformational changes by undergoing segmental torsions in the neighbourhood of the vacancy. Figure 2 shows a view along the channel direction of the PAK1 lattice which has relaxed about a K^+ vacancy, but it is typical also of the PAK2 lattice which has relaxed around a similar K^+ vacancy. The figure shows that although the square channel structure around the vacancy is retained, the PA chains constituting the channel walls lose their planarity.

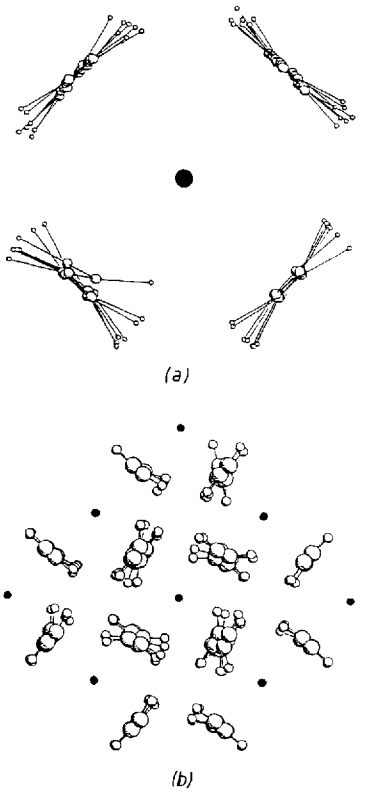

Figure 2 A view along the channel direction (*c* axis) of (a) PAK1 and (b) PAK2 which have relaxed about K^+ vacancy. The axial arrays of K^+ ions are indicated by black circles. For PAK2 portions of other channels are included to show the extent of the perturbation by the defect.

In the two structures considered the relaxations of the *dopant* sublattices show some differences. In PAK1 the defect energy and relaxed structure were found to be sensitive to the potential cutoff distance and to the size of Region I; however in PAK2 the energies and defect configuration converged to constant values as the cutoff and region size were increased. Increasing these parameters in the PAK1 defect calculations resulted in the K^+ ions K1 and K2 adjacent to the declared vacancy alternately approaching each other to eliminate the vacancy, and moving out to increase the K1...K2 gap. As a result our calculations cannot decide between these relaxation mechanisms in the PAK1 lattice.

The results of the PAK2 defect calculations unambiguously predict that in this structure the response of the dopant sublattice to the K^+ vacancy (which in the unrelaxed defect lattice would leave a gap of 9.92 Å) is a "closing of ranks" to produce a separation of 5.73 Å, as shown in Figure 3. In other words, the relaxation largely eliminates the dopant vacancy. However, the fact that the new gap is not 4.96 Å indicates either an association of the dopant for the perfect-lattice site or that the host and dopant sublattices are incommensurate.

Finally the calculations on the two structures are also distinguished by the sign of

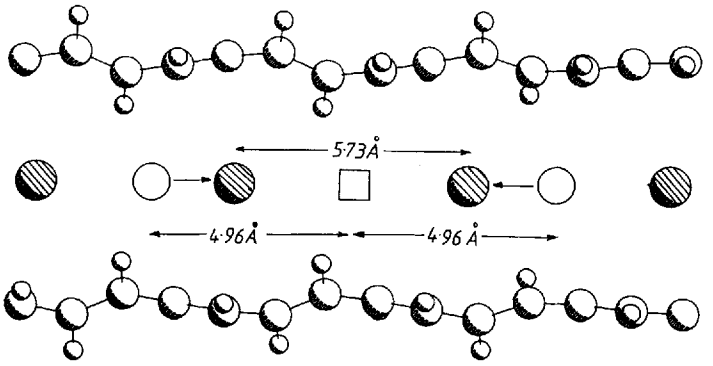

Figure 3 The relaxation of the PAK2 lattice about K^+ vacancy, the position of which is denoted by the open square. The open and shaded circles respectively represent the initial and relaxed positions of the K^+ ions in the channel.

the defect energy, which was found to be negative for PAK1 (−5.7 eV) and positive (+4.5 eV) for PAK2. The reason for the apparently negative defect energy for the former will be disussed below.

2.3 *Conclusions of K^+ Vacancy Calculations*

Since the results for the PAK2 lattice are clearer than those for PAK1 (at least for the dopant sublattice) the present work will concentrate mainly on PAK2. However the 2.48 Å dopant separation which characterises the PAK1 lattice will be discussed below. In fact the calculations on both structures seem to imply a striking mobility of the dopant ions in their channels, which just falls short of fluidity. The modification of the 9.92 Å gap by the lattice relaxation so as to produce a K . . . K separation which is little more than the PAK2 perfect-lattice separation indicates that a dopant vacancy created in this lattice is *unstable*. The fact precludes the investigation of the dopant migration through the lattice by a site-hopping mechanism such as the one that was investigated for the Li^+ ions in intercalated graphites [18, 19].

Another important result of the K^+ vacancy calcuations is the effect of the defect on the polymer sublattice. It can be seen to cause departures from the chain planarity to occur even though the relaxation, as a consequence of the near-fluidity of the dopant lattice, "repairs" the dopant sublattice so as almost to maintain its perfect-lattice spacing. Recalling that the relaxation of the perfect lattice structures using the unit cells shown in Figure 1 maintained the planarity of the PA chains in both PAK1 and PAK2, it would appear that the calculated chain distortions result from the new degrees of freedom that result from the lowering of the translational symmetry by the defect. These symmetry constraints also account for the apparent negative defect energies which were encountered above, such as those calculated for K^+ vacancy in the PAK1 lattice. The lowering of symmetry removes those constraints which prevent the polymer chains from effecting the conformational changes resulting in the relaxation of the lattices to their global energy minima. This suggests that in the *perfect lattices* of PAK1 and PAK2, the high point-group- and translational-symmetries implied by the idealised unit cells in Figure 1 impose constraints on the relaxational degrees of

freedom which the lattice simulation program CASCADE invokes to access the global energy minima.

In order to test this the atomic positions resulting from the K^+ vacancy-calculation for PAK2 were used to construct a unit cell the dimension of which in the direction of the chain was three times longer than that of the original unit cell, and performed a "perfect lattice" calculation using the enlarged unit cell. The lattice energy calculated for this structure is -485.41 eV. Since this value is less than -483.34 eV (three times the energy of the original perfect lattice) we conclude that the original unit cell was too restrictive to permit the lattice to relax to its global minimum, but that this point may be approached by removing the restrictions imposed by the translational (and perhaps point-group) symmetry of the original unit cell. In the present case this partial removal of the symmetry constrictions lowers the lattice energy (per "old" unit cell) by 0.69 eV, thereby raising the calculated defect energy to $+5.18$ eV.

Naturally the long-range order which may be investigated in this way is limited by the size of the unit cell for which it is feasible to perform the calculation. The 0.69 eV deformation-stabilization found as described here by the use of a triple cell can only be a lower limit for this energy. If, as is suggested by the dopant spacing values provided by the vacancy calculations, the host and dopant sublattices in PAK are *incommensurate* (as diffraction studies [20] have found for Cs-doped PA), a much longer unit cell would have used to simulate the structure realistically.

2.4 *Motion of K^+ Ions*

In another approach to examine the mutual distortions of host and dopant sublattices the displacement of a single K^+ ion off its perfect-lattice site in the PAK2 structure was investigated. For this defect calculation, in which there is no net vacancy or interstitial species, a K^+ ion is fixed at various positions along the axis, and the defect energy and relaxation of the lattice is monitored as the ion is advanced along the channel. It must be emphasised that this investigation of ion displacement is not intended to simulate dopant migration, for which some configuration of vacancies are almost certainly required, but to explore the "coupling" between the lattices which may be revealed by the motion.

The results of this investigation are plotted in Figure 4, which shows the variation of the relative defect energy as a function of the displacement of the selected K^+ ion which is labelled K*. The energy, starting at zero when K* is in its perfect-lattice site, becomes negative as the local lowering of the symmetry provides relaxational degrees of freedom, allowing the polymer chains to distort. Having achieved the minimum energy when relaxation is complete it increases as the ion train encounters a potential wall arising from the compression of dopant ions in the direction of its motion. The dependence of the energy on the amount of polymer distortion is shown by the dotted curve in Figure 4, which plots the root mean square (rms) displacement of the PA atoms in the unit cell from their undistorted positions, and demonstrates the necessity for the chains to distort in order to achieve maximum lattice stability. The origin of the subsequent decrease in the rms displacement is discussed below.

The sequence of channel plots in Figure 5 shows the response of the PA chains to various positions of K*, and it can be seen that the local twisting of the polymer is least in those regions in which the ions can maintain their PAK1 and PAK2 separations.

A second interesting feature of this investigation emerges from the movement of the remaining dopant ions in the vicinity of K*. Figure 5 and Table 1 show that the

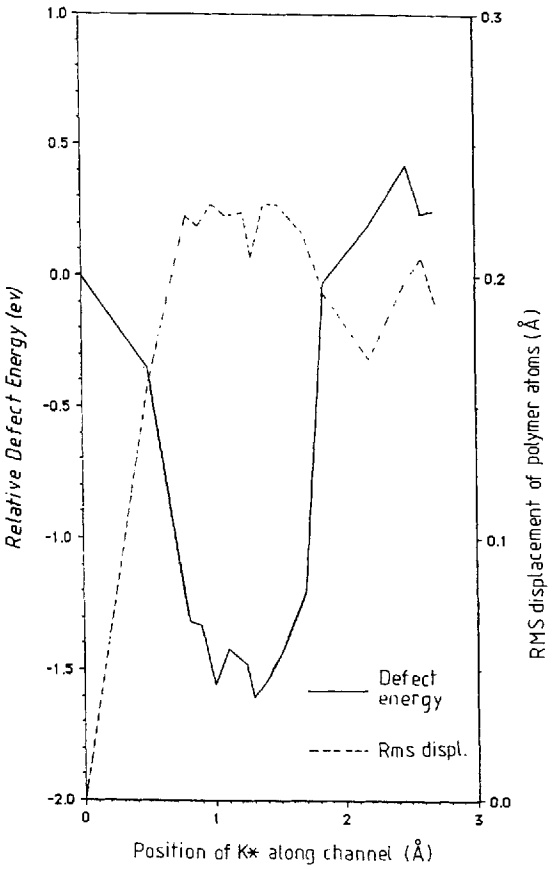

Figure 4 The "forced migration" of dopant ion K* in PAK2: the relative defect energies and root mean square displacements of polymer atoms as functions of the *c*-axial position of the K* ion.

dopant ions behind K* follow this ion, roughly maintaining the dopant sublattice repeat distance of 4.96 Å, though they increase their separation as K* approaches the exterior of the defect region, resulting in a stretching of this part of the ion train. Conversely the ions in front of K* become compressed reflecting the "potential wall" of the lattice energy. The K*...K2 separation is initially maintained at roughly the perfect lattice distance of 4.96 Å, but when K* has been displaced by 1.86 Å the separation shows an abrupt transition to values close to 2.48 Å, which is the separation in PAK1. This effect seems to indicate that although the global minimum for the $K^+ \ldots K^+$ separation in potassium-doped PA is close to the PAK2 value, there is a local minimum at half this distance, which it can assume either (a) at higher doping levels or (b) as suggested by the present results, for example, if the lattice is constricted by some defect which prevents the establishment of the PAK2-like dopant separation. This interpretation of PAK1 as a higher-energy phase of the PAK lattice suggests the possibility of coexistence of both structures in potassium-doped PA.

A comparison of Figures 4 and 5 shows that the local twisting of the polymer is least

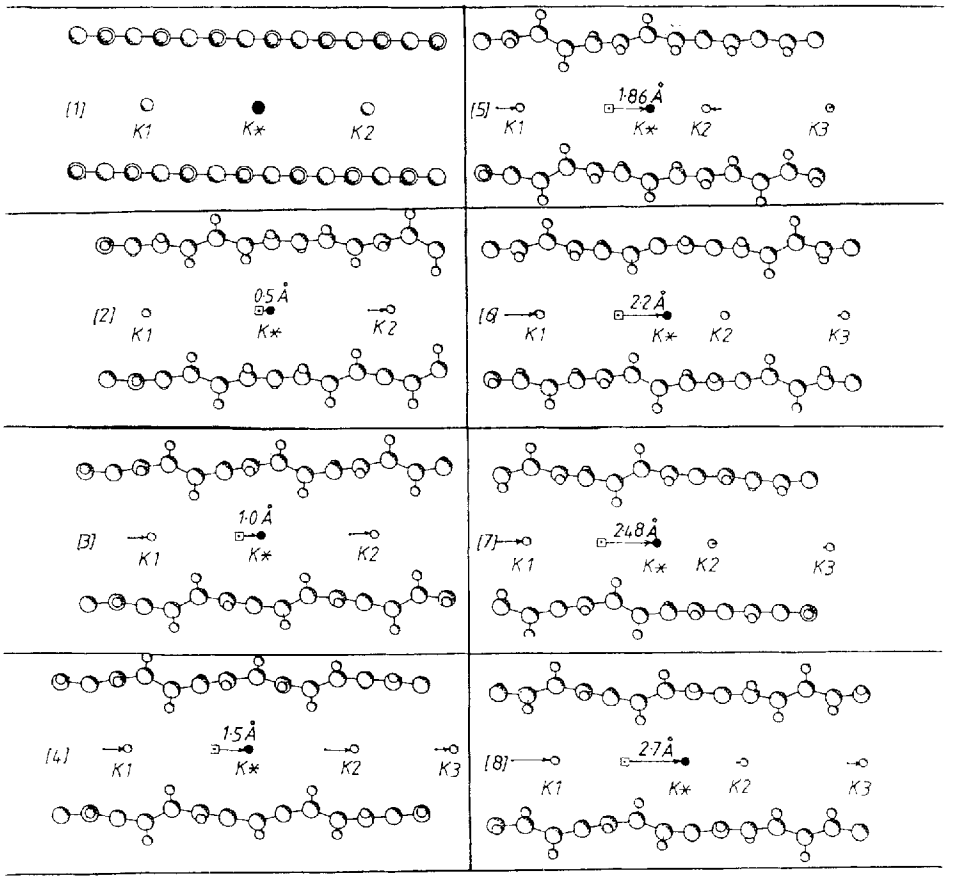

Figure 5 The "forced migration" of dopant ion K* in PAK2. The sequence [1] to [8] shows the projections of the dopant channel on to the *ac* plane for various K* displacements from the position of the perfect lattice site which is denoted by a square. The response of ion K1 "behind" and of K2 "in front of" K* are shown by the sequence.

Table 1 Separations between the migrating ions K1, K* and K2 (see Figure 4 and 5) as a function of the displacement *d* of K* from its "perfect lattice" site. All distances in Å.

d(K*)	0.0	0.5	0.8	0.9	1.0	1.1	1.24	1.3	1.4
r(K1 – K*)	4.96	5.53	4.78	4.87	4.92	5.02	5.14	5.18	5.28
r(K* – K2)	4.96	5.43	4.93	5.05	5.08	5.10	4.99	4.84	4.86
d(K*)	1.5	1.7	1.81	2.2	2.48	2.6	2.7		
r(K1 K*)	5.37	5.58	5.83	5.68	5.79	5.75	5.81		
r(K* K2)	4.78	4.57	2.49	2.57	2.45	2.61	2.57		

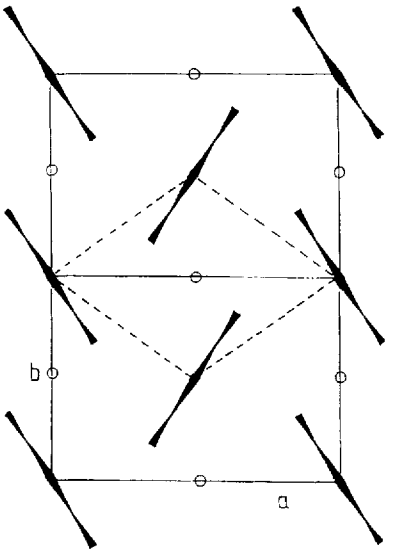

Figure 6 The unit cell of Li-doped polyparaphenylene (PPPLi), the circles indicating the dopant sites. The broken lines show the dopant channels.

in those regions in which an array of 2 or 3 adjacent ions can maintain their PAK1 and PAK2 sites or separations. When this condition is met, the relief which accrues from the deformation of the chains is reduced. This explains the increase in the energy and the decrease in the rms displacement in Figue 4 after the establishment of the PAK1 separations at the head of the moving train of ion dopants.

3 LITHIUM-DOPED POLYPARAPHENYLENE

3.1 *The Perfect Lattice*

The undoped lattice of polyparaphenylene (PPP) resembles that of polyacetylene, with two chains occupying a unit cell whose monoclinic angle is nearly 90° [9, 10]. When PPP is doped with lithium, diffraction studies have shown that Li^+ ions occupy sites along the *a* and *b* axes [9, 10], but the unit cell is otherwise hardly affected by the doping (Figure 6). Doping with potassium, on the other hand, effects more substantial changes to the pristine PPP lattice [8].

PPP doped with Li rather than with K was selected for the investigation described in this Section since the lattice defect calculations would be prohibitively slow and expensive for the PPPK lattice, which possesses a considerably larger unit cell [8].

The practice described in Section 2.1 for the PAK lattices, in which the $-e$ charge transferred from each dopant atom was distributed equally among the carbon atoms of the polymer, was followed also for PPPLi. The atom-pair and bond-angle deformation potentials used were those reported earlier [12].

The results of the diffraction investigations lead to postulated dopant sites at points halfway along both the *a* and *b* crystallographic axes as indicated in Figure 6. However, the simulation of such a "fully-doped" lattice in which all these sites were

occupied did not lead to a relaxed structure. A stable lattice could be obtained only when just *one* type of axial site (*a* or *b*) was occupied by a dopant [12].

In our simulation of the PPPLi lattice we placed the Li^+ ions on the *a* sites (such a structure is equivalent to that in which the ions occupy only the *b* sites). In this way each dopant ion was equidistant from the centres of four phenylene rings – one from each of the four chains surrounding the linear array of Li^+ ions. This lattice (Figure 6) is reminiscent of the PAK channel structure, but the polymer "walls" of the PPPLi channels are substantially twisted from the PAK square channel configuration.

3.2 *Displacement of a Dopant Ion*

When a defect calculation is performed on Li-doped PPP containing a Li^- vacancy the extent of lattice deformation is such that a stable defect structure is not obtained. It would seem that despite the apparently minimal disturbance of the host lattice by the dopant suggested by the comparison of the pristine and doped structures, those domains of the lattice which *are* doped must have the $[(C_6H_4)Li_{0.5}]_x$ structure described in Section 3.1.

In order to investigate the response of the host sublattice to displacements in the dopant channels a similar procedure as has been described for the "forced migration" of a dopant ion in PAK2 (Section 2.3) was followed. Starting from the perfect lattice structure whose *ab* and *ac* projections are shown in Figure 7, the lattice was allowed to relax around the selected migrant ion Li* as it was displaced along the channel direction (*c* axis). As soon as Li* is shifted by the smallest amount that results in a recognisable lowering of the symmetry of the unit cell the energy of the lattice begins to decrease and the PPP chains simultaneously distort, as shown in Figure 8(a). However unlike the response of the dopant K^+ ions in PAK2 to the displacement of K*, the neighbouring ions Li1 and Li2 immediately behind and in front of Li* do not remain in line with it. Li2, pursued by Li*, maintains the same *c*-axial direction as Li*, and the surrounding polymer chains are distorted relatively little. However its other neighbour Li1, following in the train of Li*, migrates in a direction normal to the channel axis (Figures 8(b) and 9), while the PPP chains in its vicinity simultaneously exhibit a disruption of the orderly packing of the perfect lattice.

These findings point to the instability of the PPPLi lattice when a dopant ion wanders too far off its site on the channel axis, between the phenylene-ring centres on the four surrounding polymer chains. The result is consistent with the failure to achieve a stable PPPLi lattice containing a Li^+ vacancy, and contrasts the attachment of the dopant ion to its site in PPPLi with the mobility of the dopants in PAK.

DISCUSSION

The contribution to the energy of doped polymer lattices arising from the deformation of the host polymer chains from chain-segment regularity is not easily obtained from a lattice simulation calculation based upon a unit cell. Merely performing a lattice relaxation in which the unit cell contains a larger number of compositional repeat units will not necessarily lead to the required deformations (even if arbitrary deformations are made to lower the point-group of the cell) since the unavoidable translational symmetry may still bar access to the correct relaxation pathway. Naturally, following the procedure in the limit of a sufficiently large cell may minimise

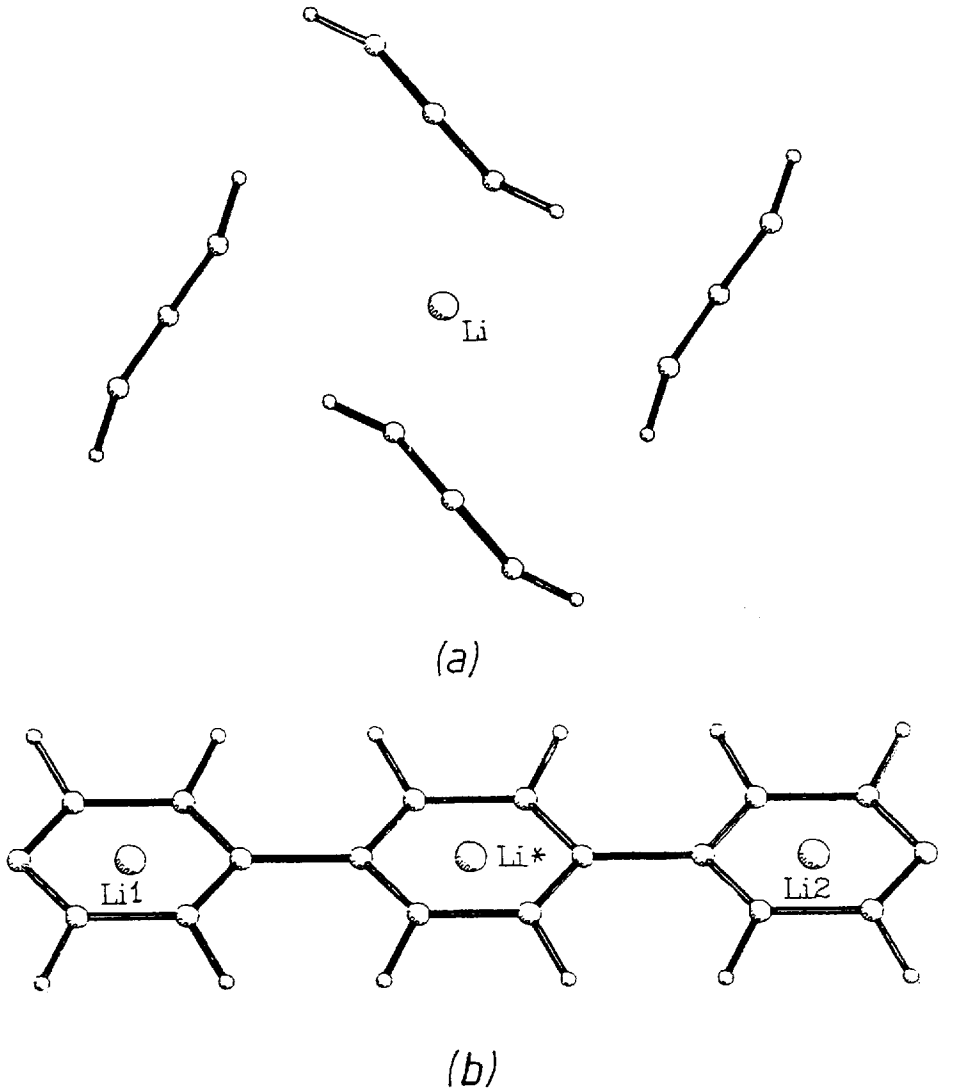

Figure 7 The dopant channel in PPPLi perfect lattice. (a) viewed along the *c*-axis, and (b) projected on to the *bc* plane.

the uncertainties, but our calculations, such as that using the PAK2 "triple cell" reported at the end of Section 2.2, suggest that this is not a reliable strategy. If components of the lattice, such as dopants in PAK, are rather mobile, the resulting incommensurability cannot be treated by a unit-cell method.

Although the host and dopant lattices in PPPLi are commensurate in so far as the Li^+ ions appear to be associated with the phenylene rings of host lattice, yet the precise description of the polymer distortions from planarity may involve an incommensurability with the rest of the lattice. In both these examples the remaining

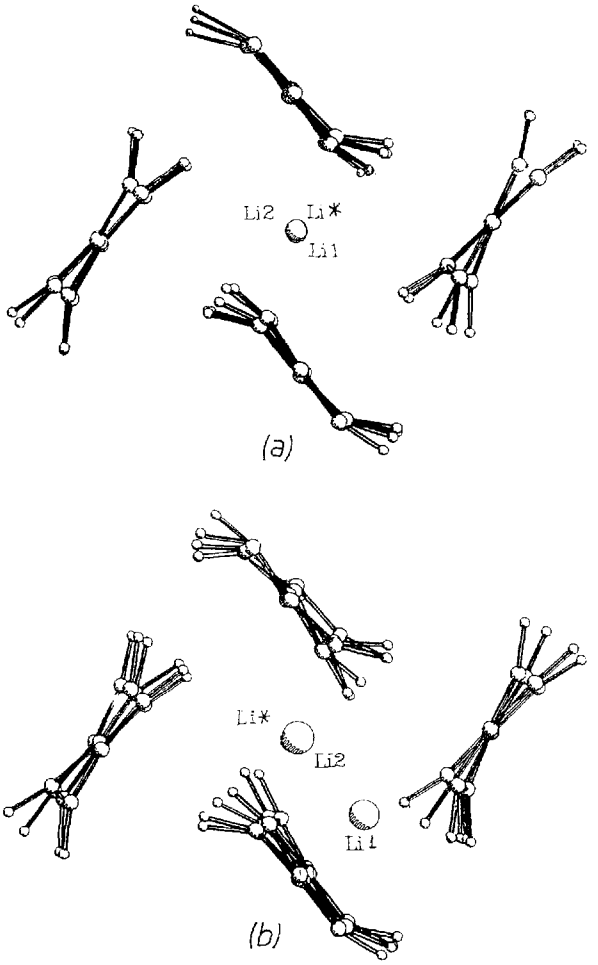

Figure 8 The response of the PPPLi lattice to the "forced migration" of dopant ion Li*, the structure viewed along a dopant channel. In (a) and (b) Li* has been displaced by 0.1 Å and 1.0 Å respectively. The axial positions of the three dopant ions Li1, Li* and Li2 are shown in Figure 9.

translational symmetry restrictions may still deny access to parts of the configurational energy surface.

One way out of the difficulty in static lattice simulation is to employ a "defective lattice" method in which the symmetry is broken by judiciously shifting atoms off their sites followed by lattice relaxation. Repeating the procedure with other sets of atomic displacements would allow the mapping of the potential energy surface.

There are as yet no experimental results to confirm the high mobility of the K^+ ions in PAK. The crystallinity and quality of samples that are currently available are limited by those of the parent pristine lattice; consequently the dopant channels are far from ideal, most of the PA chains containing no more than a few hundred carbon atoms [21]. The *c*-axis disorder thereby produced hinders the investigation of the K^+

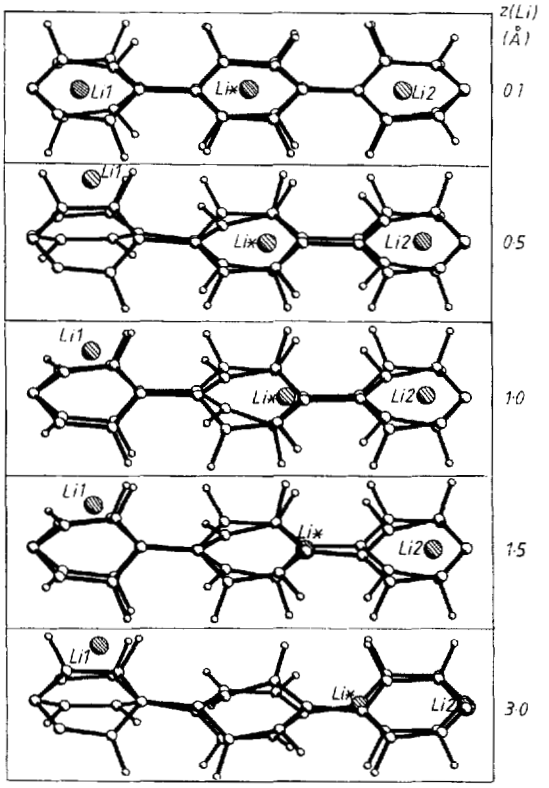

Figure 9 The response of the PPPLi lattice to the "forced migration" of dopant ion Li*, by various distances z(Li) along the dopant channel. The lattice is viewed along the a axis and includes just the two PPP chains which flank the array of dopant ions Li1, Li* and Li2.

sites on the channel. The high incidence of defects limiting the lengths of the channels caused by chain ends, cross linking, *trans* linkages etc. would be expected to result in energy barriers which would substantially decrease the mobilities of the dopants in the bulk lattice. In order to benefit from the high mobility predicted in this study for materials such as solid electrolytes it would be necessary to await the advent of highly crystalline PAK, in which systems the energy barrier for migration could be as low as 0.1 eV [22]. A recent molecular dynamics treatment of pristine and doped polyacetylenes also concludes that the dopant ions (as well as the polymer chains) are highly mobile [23].

Given the PPPLi lattice structure depicted in Figure 7, the stoichiometry $[C_6H_4Li_{0.5}]_x$ found by both compositional analysis and potentiometric measurements during the electrochemical doping [24] implies that the Li^+ ions are associated with the phenylene units. The diffraction investigations have not found reflections providing dopant separations in PPPLi, but the known strong associations between alkali metal atoms and aromatic rings makes it highly likely that the dopant sites are near the centres of the phenylene rings. Such sites have been found in PPP latices when the

dopant is potassium [8], and our present lattice simulation investigations favours such sites for the Li-doped lattice also.

The stronger host-dopant association in PPPLi than in PAK distinguishes the two doped lattices, resulting in stoichiometric commensurate sublattices in the former, while the lack of well-defined K^+ sites in PAK results in incommensurability and in mobile dopants. Another consequence of the strong host-dopant interaction in PPPLi is the apparent disruptive effect on the channel when the dopant ions move off their sites. Electrochemical studies [24] have reported transitions between $[C_6H_4Li_y]_x$ phases with $y = 1/2$, $1/3$ and $1/4$ suggesting the stability of lattices with these compostions. It would thus appear either that the perturbations observed in the simulation are not fatal to the stability of the lattice or that the dopant migration proceeds by a mechanism which is different from a simple channel translation as considered for PPPLi and PAK.

The ability of PPP chains to undergo torsion about the inter-phenylene bonds, while preserving the direction of the polymer axis, also distinguishes PPP from PA, and the closer approach of the dopant ions to the polymer in PPPLi than in the square-channelled PAK would be expected to result in a stronger host-dopant coupling.

The interactions of the Li^+ ions with the PPP rings are probably similar to those in graphite-lithium intercalates where, however, simulation shows that the lamellar nature of the host lattice allows the migration of the ions to occur with insignificant distortion of the host lattice [18, 19]. Moreover, the relative rigidity of the carbon sublattice in C_6Li and $C_{12}Li$ stabilises a large number of vacancy configurations forming the basis for migration pathways which involve predominantly the Li^+ sublattice. In PAK and PPPLi, on the other hand, the pronounced couplings between host and dopant sublattices do not permit ion migration to be described by such mechanisms.

References

[1] A.G. MacDiarmid, A.J. Heeger and P. Nigrey, U.S. Patent No. 4 321 114 (1981).
[2] F. Bénière, J. Franco and J.P. Louboutin, Fr. Patent No. 81 05568 (1981).
[3] D. MacInnes, M.A. Druy, P.J. Nigrey, D.P. Nairns, A.G. MacDiarmid and A.J. Heeger, "Organic Batteries: Reversible *n*- and *p*-type Electrochemical Doping of Polyacetylene", *Chem. Commun.*, 317–319.
[4] F. Bénière, D. Boils, H. Canépa, J. Franco, A. Le Corre and J.P. Louboutin, "Polyacetylene Solid State Batteries", *J. Electrochem Soc.*, **132**, 2100–2108 (1985).
[5] R.H. Baughman, N.S. Murthy and G.G. Miller, "The Structure of Metallic Complexes of Polyacetylene with Alkali Metals", *J. Chem. Phys.*, **79**, 515–530 (1983).
[6] J.P. Aimé, M. Bertault, P. Delannoy, R.L. Elsenbaumer, G.G. Miller and M. Schott, "Structure of K-doped Polyacetylene and its Variations with Annealing Studied by Neutron Diffraction", *J. Phys. (Paris) Lett.*, **46**, L379–385 (1985).
[7] N.S. Murthy, L.W. Shacklette and R.H. Baughman, "Effect of Charge Transfer on Chain Dimension in *trans* Polyacetylene", *J. Chem. Phys.*, **87**, 2346–2348 (1987).
[8] R.H. Baughman, L.W. Shacklette, N.S. Murthy, G.G. Miller and R.L. Elsenbaumer, "The Evolution of Structure During the Alkali Metal Doping of Polyacetylene and Polyparaphenylene", *Mol. Cryst. Lig. Cryst.*, **118**, 253–261 (1985).
[9] M. Stamm, J. Fink and B. Ticke, "Crystal Structure of Undoped and Doped Polyparaphenylene", *Mol. Cryst. Liq. Cryst.*, **118**, 281–286 (1985).
[10] M. Stamm and J. Hocker, "Structural changes in Polyparaphenylene by the Doping with AsF_5 and Alkali Metals", *J. Phys., (Paris)*, **44**, C3, 667–672 (1983).
[11] J. Corish, V.C.A. Hanratty, D.A. Morton-Blake, F. Bénière and A. Morin, "Atomistic Simulation Calculations on the Structures of Conducting Polymers. Part I: Pristine Polyacetylene and Polyparaphenylene", *J. Mol Struct.*, **207**, 41–51 (1990).

[12] J. Corish, V.C.A. Hanratty, J.-P. Margrita, D.A. Morton-Blake, F. Bénière and A. Morin, "Atomistic Simulation Investigations of the Structures of Conducting Polymers. Part II: Doped Polyacetylene and Polyparaphenylene", *J. Mol. Struct.*, **207,** 53–65 (1990); D.A. Morton-Blake, "Interatomic Potentials in Conducting Polymer Systems", *Mol. Simulation*, **4,** 285–291 (1990).
[13] J. Corish, V.C.A. Hanratty, D.A. Morton-Blake and F. Bénière, "The Motion of Ions in Potassium-Doped Polyacetylene" To be published in "*Radiation Effects*" (1991).
[14] M. Leslie, Daresbury Laboratory Rep. DS/SCI/TIMB36T, (1984).
[15] K. Soga, S. Kawakami and H. Shirakawa, "Hydrogenation of Potassium-doped Polyacetylene by Methanol", *Makromol. Chem. Rapid Commun.*, **1,** 643–646 (1980).
[16] E.J. Mele and M.J. Rice, "Semiconductor-metal Transition in Doped Polyacetylene", *Phys. Rev.*, **B23,** 5397–5412 (1981).
[17] N.F. Mott and M.J. Littleton, "Conduction in Polar Crystals. I: Electrolytic Conduction in Solid Salts", *Trans. Faraday Soc.*, **34,** 485–499 (1938).
[18] D.A. Morton-Blake, J. Corish and F. Bénière, "Lattice-Simulation Investigation of the Migration of Lithium in C_6Li", *Phys. Rev.*, **B37,** 4180–4687 (1988).
[19] J. Corish, F. Jugie, D.A. Morton-Blake, M. Leslie and F. Bénière "Lattice-Simulation Investigations of the Migration of Lithium in Intercalated Graphite", *Phys. Rev.*, **B41,** 10870–10871 (1990).
[20] J. Ma, D. Djurado, N. Coustel and P. Bernier, "X-ray Structure of Cs-doped Polyacetylene", *Phys. Rev.*, **B41,** 2971–2975 (1990).
[21] J.C.W. Chien, "Polyacetylene" (Academic Press 1984) Chapter 2.
[22] J. Corish, V.C.A. Hanratty, D.A. Morton-Blake and F. Bénière, "An Electrostatic Investigation of the Motion of Alkali Metal Cations through Polyacetylene", *Synthetic Metals*, **39,** 311–317 (1991).
[23] G. Sesé, C.R.A. Catlow and B. Vessal (to be published).
[24] L.W. Shacklette, N.S. Murthy and R.H. Baughman, "New Structural Phases of Polymer Battery Anode Materials: Alkali-metal-doped Polyacetylene and Polyparaphenylene", *Mol. Cryst. Liq.*